Above- and belowground interactions in Jacobaea vulgaris: zooming in and zooming out from a plant-soil feedback perspective

Liu, X.

Chapter 6

Distance- and density-dependent recruitment of common ragwort is not driven by plant-soil feedbacks

Xiangyu Liu[1], Dong He[2], Klaas Vrieling[1], Suzanne T.E. Lommen[1], Chenguang Gao[3], T. Martijn Bezemer[1, 4]

Affiliations

[1]Institute of Biology, Above-belowground interactions group, Leiden University, P.O. Box 9505, 2300 RA Leiden, The Netherlands

[2] College of Ecology and the Environment, Xinjiang University, China

[3]Institute of Environmental Sciences, Environmental Biology, Leiden University, Einsteinweg 2, 2333 CC Leiden, The Netherlands

[4]Department of Terrestrial Ecology, Netherlands Institute of Ecology (NIOO-KNAW), P.O. Box 50, 6700 AB Wageningen, The Netherlands

[Published in Basic and Applied Ecology 76, 1-13 (2024)]

https://doi.org/10.1016/j.baae.2024.02.003

Abstract

Aims Janzen-Connell effects state that the accumulation of natural enemies near parent plants and/or at locations where conspecifics aggregate can negatively affect its offspring. Negative plant-soil feedbacks can produce patterns of seedling performance predicted by Janzen-Connell effects and influence plant populations, but their relevance in field conditions remains unclear.

Methods Here, using spatial point-pattern analysis, we examine the spatial distribution of *Jacobaea vulgaris* to assess whether distance- and density-dependent predictions of Janzen-Connell effects are evident in the field. We established 27 replicated 8 × 8 m^2 plots at two grassland sites and mapped positions of rosette-bearing and flowering *J. vulgaris* plants within each plot. To investigate temporal distribution patterns, we tracked plant positions repeatedly in three plots during a single season. Additionally, we tested whether these patterns are soil-mediated. Soil samples were collected underneath flowering plants and at a distance of 0.5-meter, and used to compare seed germination, seedling survival, and growth under controlled conditions. Furthermore, we measured *J. vulgaris* growth in soil from patches with high *J. vulgaris* densities and soil from areas outside these patches.

Results Our findings show that density of rosette-bearing plants was lower at close distances from flowering plants than expected from null models, suggesting negative distance-dependent plant recruitment. The degree of clustering decreased over time from rosette-bearing to flowering plants, indicating density-dependent self-thinning. Seed germination was higher in soil further away from flowering *J. vulgaris* plants than in soil collected from underneath plants, but this was only true at one site. However, seedling mortality and biomass did not differ between soils collected at the two distances, and plants produced similar biomass in soil collected from inside and outside *J. vulgaris* patches.

Conclusions Our study demonstrates conspecific distance- and density-dependent plant recruitment in *J. vulgaris* in the field, but we found no evidence that this depends on belowground natural enemies.

Keywords

Jacobaea vulgaris, Janzen-Connell effects, grasslands, plant-soil interactions, point-pattern analysis, spatial seed germination

Introduction

Janzen-Connell effects state that the offspring of a plant will experience increased mortality at locations where conspecific adults have established and/or conspecifics aggregate due to the accumulation of specialized natural enemies (e.g. seed predators, herbivores and pathogens) (Janzen 1970; Connell 1971). This hypothesis suggests that negative distance- and density-dependence will promote diversity in plant communities as the transmission of natural enemies will be more effective on dominant species and therefore will prevent dominant species from competitively excluding other species (Packer and Clay 2000; Bagchi et al. 2014; Comita et al. 2014; Forrister et al. 2019). So far, Janzen-Connell effects have been confirmed in many studies primarily for tree species, but it can also play an important role in influencing plant population dynamics and plant diversity in grasslands (Mackay and Kotanen 2008; Petermann et al. 2008). However, those propositions are often based on results from pot experiments and field monocultures, and experimental evidence for Janzen-Connell effects in natural grassland communities is rare.

Herbs often accumulate natural enemies in the soil and can influence later-growing plants via plant-soil feedbacks. Negative conspecific plant-soil feedbacks, where plants grow worse in soil of conspecifics than in soil of heterospecifics, can generate patterns of seedling performance consistent with predictions of Janzen-Connell effects. Consequently, these effects can promote species coexistence and plant succession (Mills and Bever 1998; Petermann et al. 2008; Fukami and Nakajima 2013; van der Putten et al. 2013; De Long et al. 2023b). Few studies have directly tested the role of soil-dwelling natural enemies on predictions of Janzen-Connell effects for grassland species in the field (Liu et al. 2022). Instead, most studies conduct plant-soil feedback experiments with "home" and "away" soil collected from plants grown in pots or in field monocultures, and the results are then extrapolated to plant abundance in the field (Kliromonos 2002; Petermann et al. 2008; but see Kulmatiski and Kardol 2008; Kos et al. 2013; Heinze et al. 2016, 2019). However, plant-soil feedback effects measured in field collected soil from mixed plant communities may be "diluted" relative to those measured in soil conditioned by monocultures (Grenzer et al. 2021). These findings strongly emphasize the necessity of a comprehensively understanding of the role of plant-soil feedbacks in influencing plant performance and plant population dynamics.

Ecological processes such as negative density dependence can leave footprints on the spatial distribution or structure of plant species, and this is detectable by spatial point-pattern analysis (Wiegand and Moloney 2004; Velázquez et al. 2016; Ben-

Said 2021). In a spatial analysis, a plant population is represented by a set of points within a mapped area and the organization of these points in space can be used to infer ecological processes. All else being equal, if recruitment suffers from conspecific distance-dependent mortality, we would expect to observe a lower density of young plants near adult plants compared to locations far away from adult plants (Swamy et al. 2011; Murphy et al. 2017). Moreover, if a population of growing plants experiences a progressive decline in density (known as self-thinning, Westoby 1984), it is expected that young plants will exhibit a higher degree of clustering than adult plants (Getzin et al. 2008; Zhu et al. 2010; Das Gupta and Pinno 2018). For many plant species, seedling recruitment in grasslands can vary strongly within a year and highly depends on environmental factors such as precipitation (Rusch and van der Maare 1992). If seedling recruitment increases during the growth season, both the density of seedlings around adult plants and the degree of clustering among seedlings are expected to increase. Due to its elegance and power, spatial point-pattern analysis has great potential for the examination of conspecific distance- and density-dependent plant recruitment for species in dynamic mixed communities such as grasslands (De Luis et al. 2008; Zhao et al. 2020; Wang et al. 2020).

Jacobaea vulgaris (syn. *Senecio Jacobaea* L.; Asteracaea) is an early successional species that can become highly abundant in the field after disturbance (Harper and Wood 1957; van de Voorde et al. 2012b). It has been found to suffer from strong conspecific negative plant-soil feedback, and soil biota (e.g. soil fungi) have been proposed to be important drivers of this pattern (Bezemer et al. 2006; van de Voorde et al. 2011). This species is a monocarpic biennial that forms a rosette in the first year and flowers in the second year, even though flowering can be delayed e.g. due to herbivory (van der Meijden and van der Waals-Kooi 1979). It can produce large numbers of seeds (up to 30000 achenes per plant in the Meijendel, The Netherlands) (van der Meijden and van der Waals-Kooi 1979).

In this study, we investigate whether conspecific distance- and density-dependent plant recruitment are evident in *J. vulgaris* plants in two temperate grasslands in The Netherlands. Further, we examine whether the observed spatial patterns of plant recruitment are mediated by soil biota. We tested the following hypotheses:

(1) If conspecific distance-dependent plant recruitment is present in the field, the density of rosette-bearing plants near flowering *J. vulgaris* plants will be lower than expected from a random spatial distribution model.

(2) If there is conspecific density-dependent self-thinning, there will be higher spatial clustering among rosette-bearing plants than the spatial clustering between rosette-bearing plants and flowering plants, as young rosettes suffer more from density-dependent competition and/or natural enemies.

(3) Along the growing season, negative distance-based spatial patterns will become stronger, as seedling recruitment continues throughout the season and this will be inhibited nearby flowering plants.

(4) If distance-dependent effects are mediated by soil biota, plant performance will be lower in soil collected underneath flowering *J. vulgaris* plants than in soil collected away from flowering plants, this will be true in live soil and not in sterilized soil. To differentiate whether negative effects observed in underneath and away soil were due to nutrient differences in sterilized and live soil, we introduced an additional treatment with extra nutrients.

(5) If density-dependent self-thinning is soil-mediated, seedling performance will be lower in soil collected from patches with high densities of *J. vulgaris* than in soil from outside these patches.

Materials and methods

Focal plant species

Jacobaea vulgaris L., commonly known as common ragwort, is a monocarpic biennial that is native in Europe (Harper and Wood 1957). This species develops a flowering stem from May to June, and its flowers appear from July to October. Plants will die after flowering and seed set (van der Meijden and van der Waals-Kooi 1979). Seeds disperse mainly by wind and gravity (Wardle et al. 1987). Seeds can remain dormant in the soil as seed bank for many years and germinate in autumn or spring (van der Meijden 1979).

Study sites and spatial data recording

To investigate the spatial distributions of rosettes and flowering *J. vulgaris* plants, a total of 27 plots measuring 8 × 8 m each were established and monitored in two natural grasslands. Fifteen plots were established in a grassland of around 300 m × 100 m in Meijendel (52°07' N, 4º20' E) a coastal dune region (Fig. 6.1 A) where *J. vulgaris* was present. The distance between each plot was at least 50 m at Meijendel. The population of *J. vulgaris* plants in this area exhibits significant fluctuations over years, with average cover ranging from 14% to 0.5% (van der Meijden, 1979). The sandy dune soil at Meijendel is known to have limited nutrient availability (Gao 2023). Twelve plots were established in a natural grassland on a former arable field "Mosselse Veld" (where agricultural practices stopped in 1985) at the Veluwe area in the central part of the Netherlands (52°04' N, 5º44' E) (Fig. 6.1 A). Details about the sampling and site are described elsewhere (Kos et al. 2013). In brief, within a 400 × 100 m grassland, 8 × 8 m plots were established in areas where *J. vulgaris* was present, with a minimum distance of 80 m between plots. Plant species richness at Mosselse Veld was 15 species per m^2 on average, and the average cover of *J. vulgaris* was 6% (Kos et al. 2013). The soil was a sandy loam soil and soil abiotic characteristics varied between plots (Kos et al. 2013). Concentrations of soil nutrients were higher at Mosselse Veld than at Meijendel (see Supporting information: Table S.6.1).

Data were collected in 2010, 2020 and 2021 (see Supporting information: Table S.6.2). Each plot was subdivided into 64 sub-plots of 1 × 1 m^2 (Fig. 6.1 C and D) and each subplot was further divided into sixteen 0.25 × 0.25 m^2 cells (Fig. 6.1 C and D). The location of each rosette and flowering *J. vulgaris* was recorded on grid

paper (Fig. 6.1 D, plot 16 in August 2010 at Mosselse Veld). The abundance of *J. vulgaris* ranged from 118 to 1755 per plot at Meijdendel, and from 86 to 903 per plot at Mosselse Veld (see Supporting information: Table S.6.2). In addition, the rosette diameters of all young and flowering plants were measured and recorded in plot 1-8 in June 2020 at Meijdendel. At Meijendel we observed that during the growth season, new seedlings of *J. vulgaris* emerged. To capture the temporal dynamics of spatial patterns of rosettes and flowering plants, we monitored three plots at Meijendel during the growth season in 2020, with plants recorded in late May, mid-July, and late August (see Supporting information: Table S.6.2). In the plots that were investigated in late May 2020, *J. vulgaris* plants were not yet flowering and we used the maps of flowering plants in July and August to identify the flowering plants of the first investigation.

Soil bioassay 1: testing for the soil-mediated distance-dependent effect

In June 2021, 30 flowering *J. vulgaris* plants were randomly selected at each of the two locations. The height of the flowering plants was recorded. We collected soil (3 cores, 5 cm diameter, 5 cm depth) underneath each flowering plant (*J. vulgaris* rhizosphere soil). A paired "away" soil sample was collected at 50 cm distance in a random direction and ensuring there were no other *J. vulgaris* plants nearby this away sample (Fig. 6.1 E). In total, 120 soil samples (2 sites × 30 flowering plants × 2 soil types) were collected. Each soil sample was homogenized and gently sieved through a 1 cm sieve to remove stones and moss. Then, soil samples were stored at 4 °C until further use. To test for soil-mediated distance dependent effects on plant growth and to examine whether this effect was related to nutrient deficiency in the soil or due to soil-borne pathogens, we conducted an experiment where plants were grown in microcosms (10 cm height, 2.5 cm diameter) filled with 10-gram of soil (Fig. 6.1 E). For each soil sample 9 microcosms were filled with soil. Three microcosms were autoclaved for 1 h to sterilize the soil (hereafter, sterilized soil). Three microcosms received 5 ml of sterilized water (hereafter, live soil), and the final set of three microcosms received 5 ml of Steiner nutrient solution which is widely used in plant growth experiments (hereafter, live soil + nutrients) (Steiner, 1968; Joosten et al. 2009; Zhang et al. 2022a). The chemical composition of the Steiner nutrient solution that was used is shown in the Appendix (Supporting information: Table S.6.3). One surface sterilized *J. vulgaris* seed was then placed on top of the soil in each microcosm. *J. vulgaris* seeds were collected from Meijendel in September 2020. Seeds were surface-sterilized by soaking in 5% sodium hypochlorite for 20 min and rinsed three times with sterilized MillQ water. In total, there were 1080 microcosms (30 plants × 2 types × 2 sites × 3 treatments

× 3 replicates = 1080 microcosms). Each microcosm was covered with a transparent plastic lid (2.65 cm height, 2.65 cm diameter). Microcosms were randomly placed in a tray in the climate chamber at 16/8 h light-dark regime and a 20/15 °C temperature regime and RH = 70%. Seed germination was recorded for each microcosm every three days. 80% of the seeds germinated within 7 days. Seedling mortality was recorded regularly. Four weeks after adding the seeds, the surviving seedlings were harvested. Roots were washed to remove soil and plants were oven-dried at 70 °C and total biomass per plant was recorded. The mean plant-soil feedback effect for each flowering *J. vulgaris* plant was then calculated with the following formula: ln (plant dry mass in underneath soil / plant dry mass in away soil) (Petermann et al. 2008; Brinkman et al. 2010; Bezemer et al. 2018).

Seed bank experiment

To avoid the confounding effects of the seed bank, we also determined the seed germination of *J. vulgaris* from the seed bank in "underneath" and "away" soil collected for soil bioassay 1 (Fig. 6.1 E). Microcosms were filled with 10 g of soil from each sample. Each microcosm received 5 mL water and was covered with a transparent plastic lid and kept under conditions as described above. Microcosms were checked regularly and germinated seedlings were identified and then gently removed with a tweezer. The number of *J. vulgaris* seedlings in each microcosm was recorded. There were three replicate microcosms for each soil sample and a total of 360 microcosms (2 sites × 30 flowering plants × 2 soil types × 3 replicates).

Soil bioassay 2: testing for the soil-mediated density-dependent effect

In March 2010, we examined whether the performance of *J. vulgaris* in soil collected from patches with high densities of *J. vulgaris* plants differed from that in soil collected outside these patches (Fig. 6.1 F). This was done with soil samples collected from natural grassland at the Veluwe area near Mosselse Veld: Reijerscamp (52°00' N, 5°47' E), a former arable site where agricultural practices stopped in 2005. Sterilized *J. vulgaris* seeds were germinated in containers (10 × 10 × 4 cm) filled with a layer of sterilized glass beads submerged in water in a climate chamber at 16/8 h light-dark regime and a 20/15 °C temperature regime. Seeds were collected from Mosselse Veld in September 2009. After germination, seedlings were stored at 4 °C until further use. Soil was collected from 17 patches (Mean ± SE of the patch size: 8.53 ± 0.80 m^2) with high densities of flowering *J. vulgaris* plants over an area of 400 × 400 m grassland. The distance

between two patches was around 80 meters. Soil samples (10 cores, 5 cm diameter, 15 cm depth) were collected in a 1 × 1 m^2 plot inside each patch and an adjacent 1 × 1 m^2 plot outside the patch. The number of *J. vulgaris* stems in each 1 × 1 m^2 plot was also recorded (see Supporting information: Table S.6.4). *J. vulgaris* stem density, mean height of the stems, number of rosettes (measured in May 2010), and percentages of bare soil and moss were also measured (see Supporting information: Table S.6.4). Each soil sample was homogenized and gently sieved through a sieve (1 cm mesh size). Homogenized bulk soil, collected from the same area and sterilized with gamma radiation (> 25KGray, Isotron, Ede, The Netherlands), was mixed with the soil samples in a 1:6 ratio (live/sterilized). Pots (13 cm × 13 cm × 13 cm) were filled with l liter of the soil mixtures. Three *J. vulgaris* seedlings were planted in each pot and there were three replicate pots for each soil sample (Fig. 6.1 F). In total 102 pots were used (17 patches × 2 density treatments × 3 replicates). Seedlings that died during the first week were replaced. The pots were placed randomly on three trolleys (3 blocks). Each block contained one replicate of the 34 samples. The position of the trolleys was regularly changed. In the greenhouse climatic conditions were controlled and light, humidity and temperature (16/8 h light-dark regime, 20/15 °C temperature regime and RH = 70%) were equal for all pots during the experiment. Plants were watered three times per week and soil moisture content was regularly equalized during the course of the experiment by weighing pots and adding water appropriately. Eight weeks after planting, for each pot shoots were clipped and roots were rinsed with tap water to remove adhering soil. Shoot and root material was then oven dried (70 °C, 48 h), and plant dry-mass was determined.

Data analysis and statistics

Spatial pattern analysis for conspecific distance-dependent effects

The O-ring analysis was used to examine conspecific distance-dependent plant recruitment of *J. vulgaris* in the field (Wiegand and Moloney 2004). The O-ring statistic is defined as following formula:

$O(r) = \lambda \times g(r)$

Where λ the point density of the pattern, and $g(r)$ is the pair correlation function, describing the mean number of points at distance r from the set of focal points independent of the intensity λ.

The pair correlation function is defined as:

$g(r) = (2\pi r)^{-1} \times dK(r) / dr$

Where *K(r)* is the expected number of points within a circle of radius *r* centered at a point, normalized by the intensity λ of the pattern (Ripley's *K* function). As the derivative of *K(r)*, the function *g(r)* separates broad-scale patterns from successively cumulative short-scale patterns (Wiegand and Moloney 2004). So that "the O-ring statistic estimates the mean number of neighboring individuals within an annulus of radius r and width *w* around a typical point of the pattern" (Wiegand and Moloney 2004). In the case of our study, it can be used to quantify the density of rosette-bearing plants around flowering *J. vulgaris* at varying distances. The analyses were carried out for each of the 27 plots.

To investigate whether the distribution of flowering plants (pattern 1) restrict that of rosette-bearing plants (pattern 2) at somewhere far away, the appropriate null model is to randomize the locations of rosette-bearing plants while keeping the locations of flowering plants fixed (Velázquez et al. 2016). This is also known as antecedent conditions, in which pattern 1 influences pattern 2, but not the other way around. Because rosette-bearing plants in the 8 × 8 m^2 plots do not follow a homogenous Poisson distribution, rosette-bearing plants were randomized following a heterogeneous Poisson process. Here, we employed a Gaussian smoothing kernel to directly estimate the intensity function λ (x, y) from the observed data (Wiegand and Moloney 2004). We constructed the intensity function λ (x, y) using a bandwidth R = 1.0 m, as the median dispersal distance of *J. vulgaris* seeds is typically within 1 m (McEvoy and Cox 1987; Wang et al. 2020). Based on a study of objects of finite size using spatial point-pattern analysis i.e. shrubs (Wiegand et al. 2006), we set the ring-width *w* to 0.02 m in our study. In the null models, rosette-bearing plants were spatially randomized with exactly the same density as observed in each plot. Significant departure from the null expectation (i.e., $O(r) = \lambda(r)$) was evaluated using the 5^{th}-lowest and 5^{th}-highest *O(r)* statistics out of 99 simulations (95% simulation envelopes). The aggregation of rosette-bearing plants around flowering *J. vulgaris* for each distance class (from 0 to 1 m with 0.02 m increments) was calculated. Positive values indicate positive association patterns, while negative values indicate segregation patterns. This analysis was conducted using the grid-based software Programita (Wiegand and Moloney 2014).

To compare the aggregation of rosette-bearing plants around flowering *J. vulgaris* over different plots at the two sites, we used the method described by Graff and Aguiar (2011). The *O(r)* values for each plot were transformed to the weighted *O(r)* as follows:

If *O(r)* > upper 95% confidence limit (CL+), then the weighted *O(r)* = (*O(r)* - CL+) / CL+ (values larger than 0)

If *O(r)* < lower 95% confidence limit (CL−), then the weighted *O(r)* = (*O(r)* - CL−) / CL− (values smaller than 0)

If *O(r)* is in between the upper 95% and the lower 95% confidence limit (CL−), then the weighted *O(r)* = 0.

Conspecific density-dependent thinning

Density dependent competition and accumulation of pathogens can result in mortality which thins the aggregated plants (self-thinning) and increases the distance between neighboring plants (Moeur 1997). To infer the effect of density-dependent thinning from rosette-bearing to flowering stage, we used a case control approach (Getzin et al. 2008). The detailed information regarding this method can be found in the Supporting information. In brief, we categorized flowering plants as controls (pattern 1) and rosette-bearing plants as cases (pattern 2). Subsequently, we examined the difference between the mean number of rosette-bearing plants around a flowering *J. vulgaris* and that around a rosette-bearing plants at distance *r*, denoted as $g_{21}(r)$ and $g_{22}(r)$, respectively. If $g21(r) - g22(r) < 0$, this indicates that the case pattern (rosette-bearing plants) shows additional aggregation independent of the control pattern (flowering plants), reflecting a density-dependent thinning process. When $g21(r) - g22(r) < 0$, the scale *r* reflects the spatial scales at which density-dependent thinning takes place, and the radius with the maximum difference (r_{max}) corresponds to the scale at which the strength of density dependent thinning culminates (Zhu et al. 2010). Linear regression was then used to examine the relationship between the total density of *J. vulgaris* plants (rosette-bearing plants and flowering plants) and r_{max} at plot level.

To test for any departure of the case pattern from the control one, we used the local random labelling method as the null model. This approach is advantageous for removing the larger-scale effects on density of rosette-bearing plants, such as environment filtering processes (Wiegand and Moloney 2014; Velázquez et al.

2016). Specifically, we kept the locations (coordinates) of all plants as observed, but randomly assigned labels of rosette-bearing plants to locations of all plants within a 1-m scale based on the aforementioned seed dispersal range (McEvoy and Cox 1987; Wiegand and Moloney 2014). The difference between $g_{21}(r)$ and $g_{22}(r)$ was recalculated in each simulation. Significant departure from the null expectation (i.e. $g_{21}(r) - g_{22}(r) = 0$) with local random labelling was evaluated through the 95% confidence intervals of randomly-generated case-control differences in 99 simulations. This analysis was conducted using the grid-based software Programita (Wiegand and Moloney 2014). To compare the degree of self-thinning for *J. vulgaris* over plots, we used the method akin to weighted $O(r)$ as described above. To examine whether rosette-bearing plants are smaller than expected near flowering plants, we used the mark correlation function to analyze the diameter of rosette-bearing plants around flowering plants at distance r (Illian et al. 2008; Wiegand and Moloney 2014; Velázquez et al. 2016). Detailed information regarding this method can be found in the supplementary materials.

Soil bioassay 1:

Seed germination, seedling mortality and biomass: The effects of the soil type (underneath or away), soil treatment (sterilized soil, live soil, or live soil with nutrients) and their interaction on germination (yes/no) were tested using generalized linear mixed models with a binomial distribution. Analyses were done separately for the two sites. Flowering plant ID was added as a random effect. The significance of factors was assessed by comparing models with and without the factor using a Chi-squared Likelihood Ratio (LR) test and by comparing the residual deviance. Generalized linear mixed models with a binomial distribution were performed using the "glmer" function with the "lme4" package (Bates et al. 2015). The effects of soil type, soil treatment and their interaction on seedling mortality and total dry mass were tested by a two-way ANOVA with soil type and soil treatment as main factors for each site. A Tukey's post-hoc test was used for pair-wise comparisons of soil type and soil treatment. The relationship between mean plant-soil feedback effects and the height of flowering *J. vulgaris* plants was examined with linear regression using the "lm" function in R.

The difference in the number of seedlings of *J. vulgaris* that emerged from the seed bank in the underneath soil and the away soil was tested using a generalized linear mixed model with a binomial distribution and with flowering plant ID as the

random effect for each site. As none of the microcosms had more than one seedling presence/absence was analyzed.

***Soil bioassay 2**:*

The effects of the origin of the soil (inside or outside the patch) on individual shoot dry mass, total shoot dry mass and total root dry mass of *J. vulgaris* were analyzed using a pairwise t-test with the patch treatment (inside/out) as factor. ANOVA tests were carried out with the "aov" function and post-hoc tests were performed using the "glht" function with the "multcomp" package (Hothorn et al. 2008). In all analyses, residuals were checked for homogeneity of variance using a Levene's test and normality by a Shapiro Wilk test. The Levene's test and Shapiro Wilk test were performed using the "levene_test" and "shapiro_test" functions with the "rstatix" package (Kassambara 2022). Plant dry mass was square-root transformed to fulfil requirements of normality.

All analyses were performed using the R statistical language, version 4.0.4 (R Core Team 2022) and the grid-based software Programita (Wiegand and Moloney 2014).

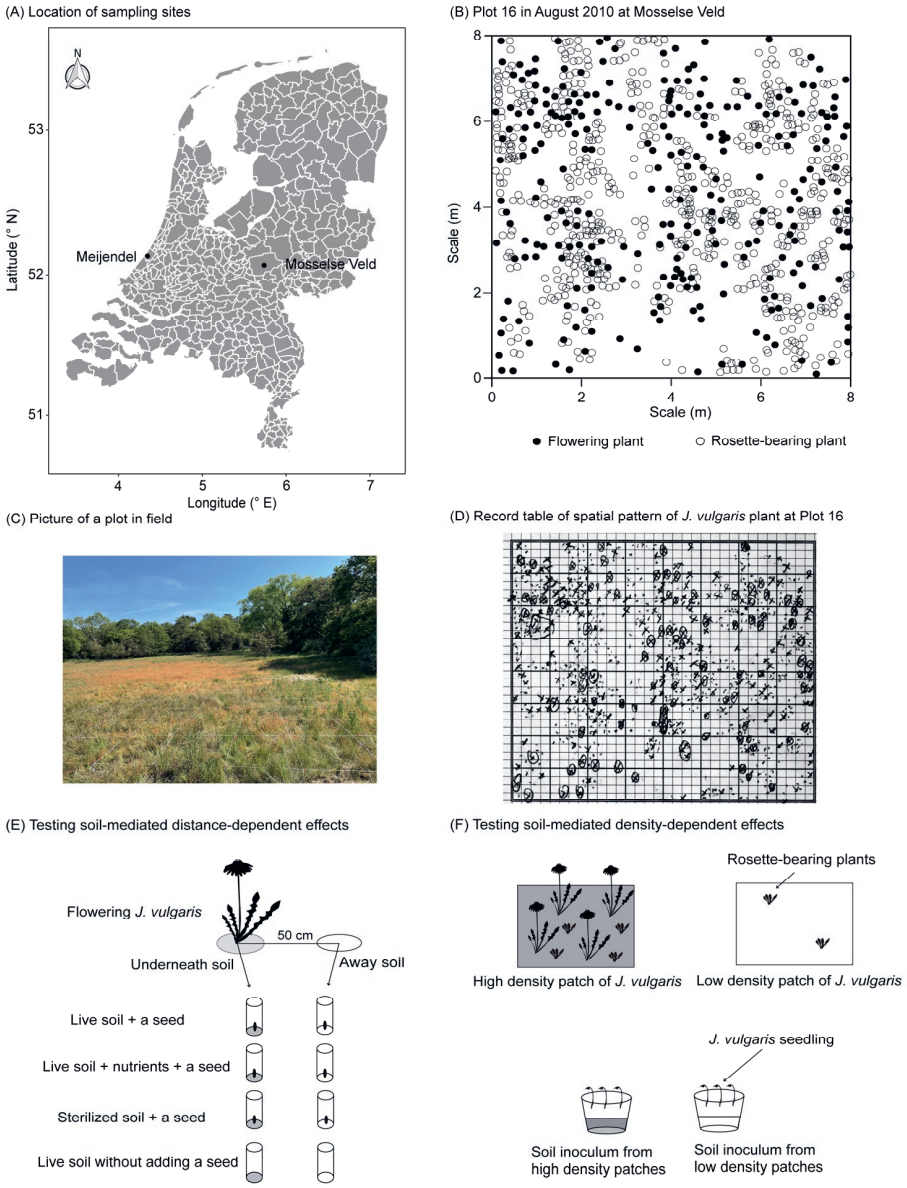

Fig. 6.1. Location of the sampling sites in The Netherlands (A), spatial distribution of rosette-bearing (open dots) and flowering *J. vulgaris* plants (black dots) at plot 16 at Mosselse Veld (B), picture of a 8 × 8 m^2 plot at Meijendel (C), map of coordinates of rosette-bearing (dots) and flowering plants (cross) in a 8 × 8 m^2 plot (plot 16 at Mosselse Veld) (D), experimental design of testing for soil-mediated distance-dependent effects (E) and design of testing for soil-mediated density-dependent effects (F).

Results

Distance-dependent spatial patterns

The neighborhood density of rosette-bearing plants around flowering plants at the two sites overall showed similar patterns but the patterns also varied between years (Fig. 6.2). The observed density of rosette-bearing plants near flowering plants was lower than expected from null models (a segregated pattern of rosette-bearing and flowering plants) (Fig. 6.2). This was evident for more than half of the plots at Meijendel in 2020 (n = 11, 6 out of 11) and for all plots in 2021 (n = 4, all 4) (Fig. 6.2 A and C), and for more than 50% and 75% plots at Mosselse Veld in 2010 (n = 8, 4 out of 8) and 2021 (n = 4, 3 out of 4) respectively (Fig. 6.2 B and D). The segregated pattern was present at 0 – 8 cm (2020) and 0 – 20 cm (2021) at Meijendel, and at 0 – 14 cm (2010) and 0 – 20 cm (2021) at Mosselse Veld (Fig. 6.2).

Density-dependent self-thinning

The percentage of plots that showed density-dependent thinning of rosette-bearing plants, varied between sites and years (Fig. 6.3). At Meijendel, in June 2021, more than half of the plots showed density-dependent thinning (n = 4, black area in Fig. 6.3 A), while in June 2020 this was true for around 20% of plots (n = 11; Fig. 6.3 C). At Mosselse Veld, all plots (n = 4) in 2021 and 75% (n = 8) of plots in 2010, showed density-dependent thinning (Fig. 6.4 B and D). Among plots, the distance to flowering plants at which the strength of density-dependent thinning peaked was not correlated to the density of *J. vulgaris* at the plot level (see Supporting information: Fig. S.6.2).

During the growth season in 2020 at Meijendel, the density of rosette-bearing plants increased and the segregation pattern of rosette-bearing plants and flowering plants at fine scales increased (Fig. 6.4; see Supporting information: Table S.6.1). Specifically, there was no spatial association between rosette-bearing plants and flowering plants in late May, but there was in July and August 2020 (Fig. 6.4 A, C and E). Along the growth season, a self-thinning pattern of rosette-bearing plants emerged (Fig. 6.4 B, D and F). Moreover, the observed mean diameter of rosette-bearing plants nearby flowering plants did not differ from the expectation of the null model (see Supporting information: Fig. S.6.1).

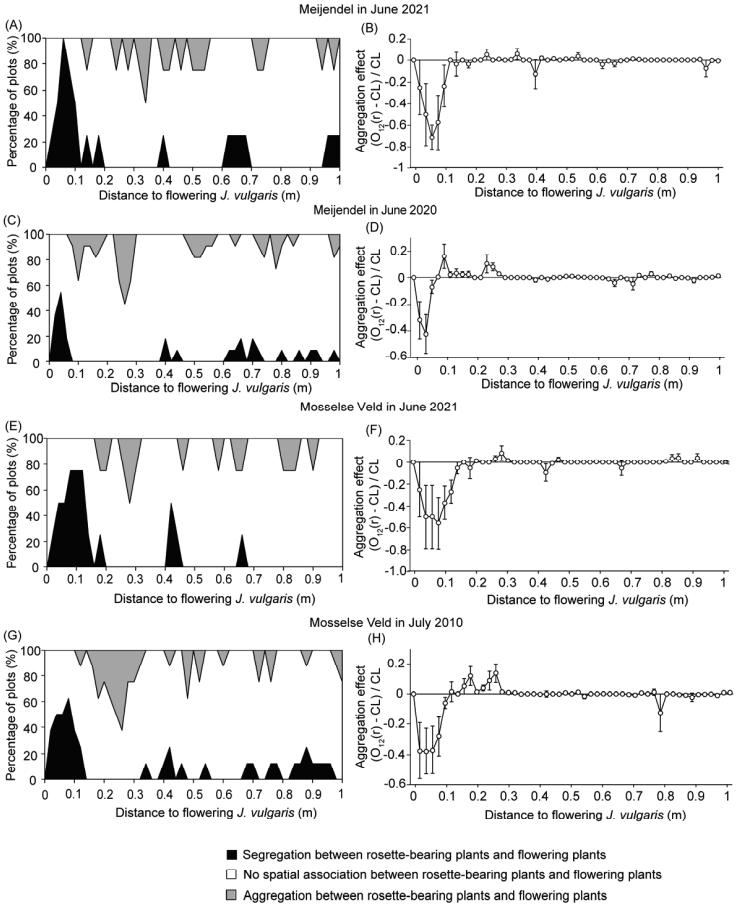

Fig. 6.2. Percentage of plots where the neighborhood density of rosette-bearing plants at distance r (m) to flowering *J. vulgaris* plants ($O_{12}(r)$) are lower than expected from null models, do not deviate from expected from null models or are higher than expected from null models, and mean (± SE) relative spatial association of rosette-bearing and flowering plants based on the weighted O-ring function analysis. A and B show results for June 2021 at Meijendel (n = 4); C and D show results for June 2020 at Meijendel(n = 11); E and F show results for June 2021 at Mosselse Veld (n = 4); G and H show results for July 2010 at Mosselse Veld is presented (n = 8). The antecedent condition null model (Wiegand and Moloney 2004) randomizes the locations of rosette-bearing plants (pattern 2) and keeps the locations of flowering plants fixed (pattern 1). In (A), (C), (E) and (G) the black area indicates the percentage of plots that shows segregation (values below the lower limits of the 95% confidence interval), the white area indicates the percentage of plots with no spatial association (values in between the 95% confidence interval), and the light grey area indicates the percentage of plots that shows aggregation (values above the higher limits of the 95% confidence intervals). In (B), (D), (F) and (H) negative values indicate segregation, positive values indicate aggregation, and zero indicates no spatial association between rosette-bearing and flowering plants.

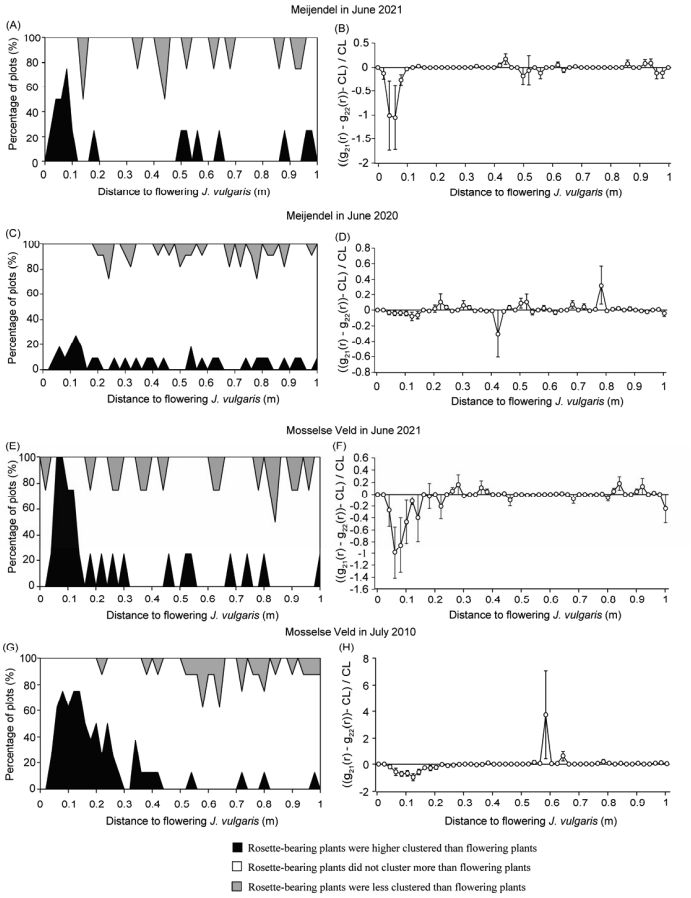

Fig. 6.3. Self-thinning effects at distance r (m) to flowering *J. vulgaris* plants and mean (± SE) relative self-thinning effect results from the weighted $g_{21}(r) - g_{22}(r)$ function analysis. A and B show results for June 2021 at Meijendel (n = 4); C and D show results for June 2020 at Meijendel (n = 11); E and F show results for June 2021 at Mosselse Veld (n = 4); G and H show results for July 2010 at Mosselse Veld (n = 8). We used the local random labeling null model (rosette-bearing plants were not moved more than 1m) to access spatial correlation of rosette-bearing and flowering plants at fine scales. In (A), (C), (E), and (G) the black area indicates the percentage of plots where rosette-bearing plants were more clustered than flowering plants which represents self-thinning of plants ($g_{21}(r) < g_{22}(r)$ below the lower limits of the 95% confidence interval), the white area indicates the percentage of plots where rosette-bearing plants did not show more clustering than flowering plants ($g_{21}(r) < g_{22}(r)$ in between the 95% confidence interval), the light grey area indicates the percentage of plots where rosette-bearing plants were less clustered than flowering plants ($g_{21}(r) > g_{22}(r)$ above the higher limits of the 95% confidence interval). In (B), (D), (F) and (H) negative values indicate self-thinning of plants, positive values indicate rosette-bearing plants were less clustered than flowering plants, and zero indicates rosette-bearing plants did not cluster more than flowering plants.

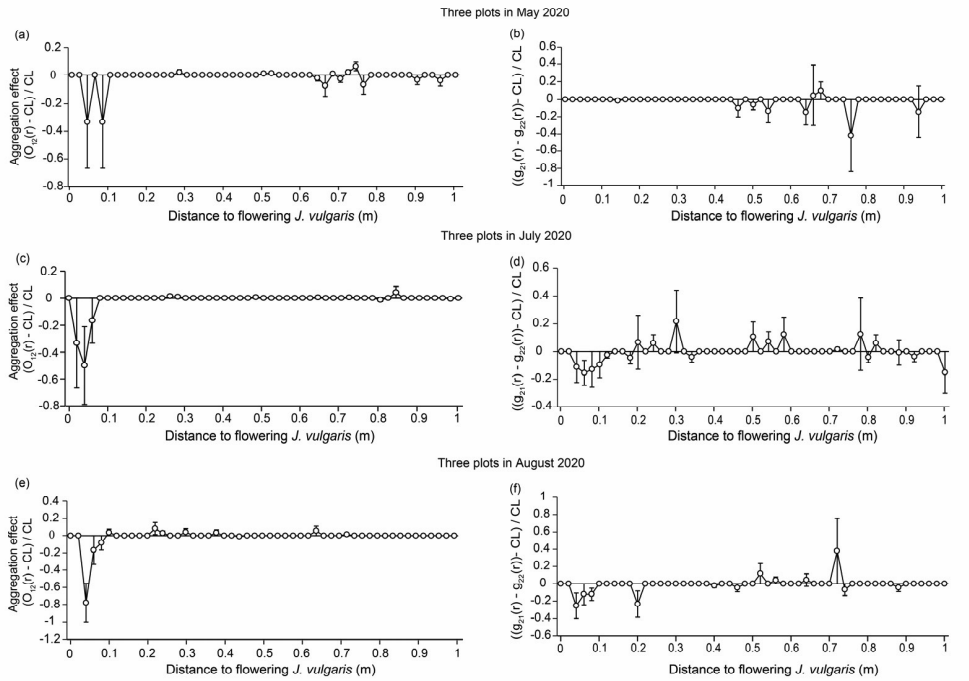

Fig. 6.4. Mean (± SE) relative spatial association of rosette-bearing and flowering *J. vulgaris* plants resulting from the weighted O-ring function analysis (A, C, E) and relative self-thinning effects resulting from the weighted $g_{21}(r) - g_{22}(r)$ function analysis (B, D, F) in 3 temporal plots in 2020 at Meijendel. In (A), (C) and (E), the antecedent condition null model (Wiegand and Moloney 2004) randomizes the locations of rosette-bearing plants (pattern 2) and keeps the locations of flowering plants fixed (pattern 1). Negative values indicate segregation, positive values indicate aggregation, and zero values indicate no spatial association. In (B), (D) and (F), the local random labeling null model (rosette-bearing plants were not moved more than 1m) to access spatial correlation of rosette-bearings and flowering plants at fine scales. Negative values indicate self-thinning of plants, positive values indicate that rosette-bearing plants were less clustered than flowering plants, and zero values indicate that rosette-bearing plants did not cluster more than flowering plants.

Seed germination and *seedling survival in soil bioassay 1*

There was no difference in the proportion of microcosms that contained a germinating *J. vulgaris* seedling from the seed bank between underneath and away soil (Meijendel: $\chi 2 = 0.96$, $P = 0.33$; Mosselse Veld: $\chi 2 = 1.25$, $P = 0.26$; see Supporting information: Fig. S.6.3). The proportion of microcosms where the added seed germinated was higher in away soil than in underneath soil, but this was

only true for soil samples from Mosselse Veld (Fig. 6.5 A and B; see Supporting information: Table S.6.4). The proportion of microcosms with a germinated seedling varied significantly among the three soil treatments, but only at Meijendel, where it was lower in the sterilized soil than in the live soil (Fig. 6.5 A; see Supporting information: Table S.6.4). There was no difference in seedling mortality between underneath soil and away soil at both sites (Fig. 6.5 C and D; see Supporting information: Table S.6.4). However, mortality of the germinated seedlings at Meijendel, was higher in live soil with addition of nutrients than in sterilized soil (Fig. 6.5 C; see Supporting information: Table S.6.4).

Plant biomass in the soil bioassays

Seedling biomass did not differ in underneath soil and away soil at both sites (Fig. 6.5 E and F; see Supporting information: Table S.6.5). There was no difference in seedling biomass among soil treatments (Fig. 6.5 E and F; see Supporting information: Table S.6.5). Flowering *J. vulgaris* plants were taller at Mosselse Veld (Mean ± SE: 42.37 ± 1.75 cm) than at Meijendel (Mean ± SE: 75.43 ± 1.93 cm) ($F_{1, 58} = 31.51$, $p < 0.001$), but there was no relationship between mean plant-soil feedback effects and the height of flowering *J. vulgaris* plants (see Supporting information: Fig. S.6.4). In the pot experiment with soil from inside and outside patches with flowering *J. vulgaris* plants, plants produced similar biomass in the soil from inside and outside of these patches (see Supporting information: Table S.6.6).

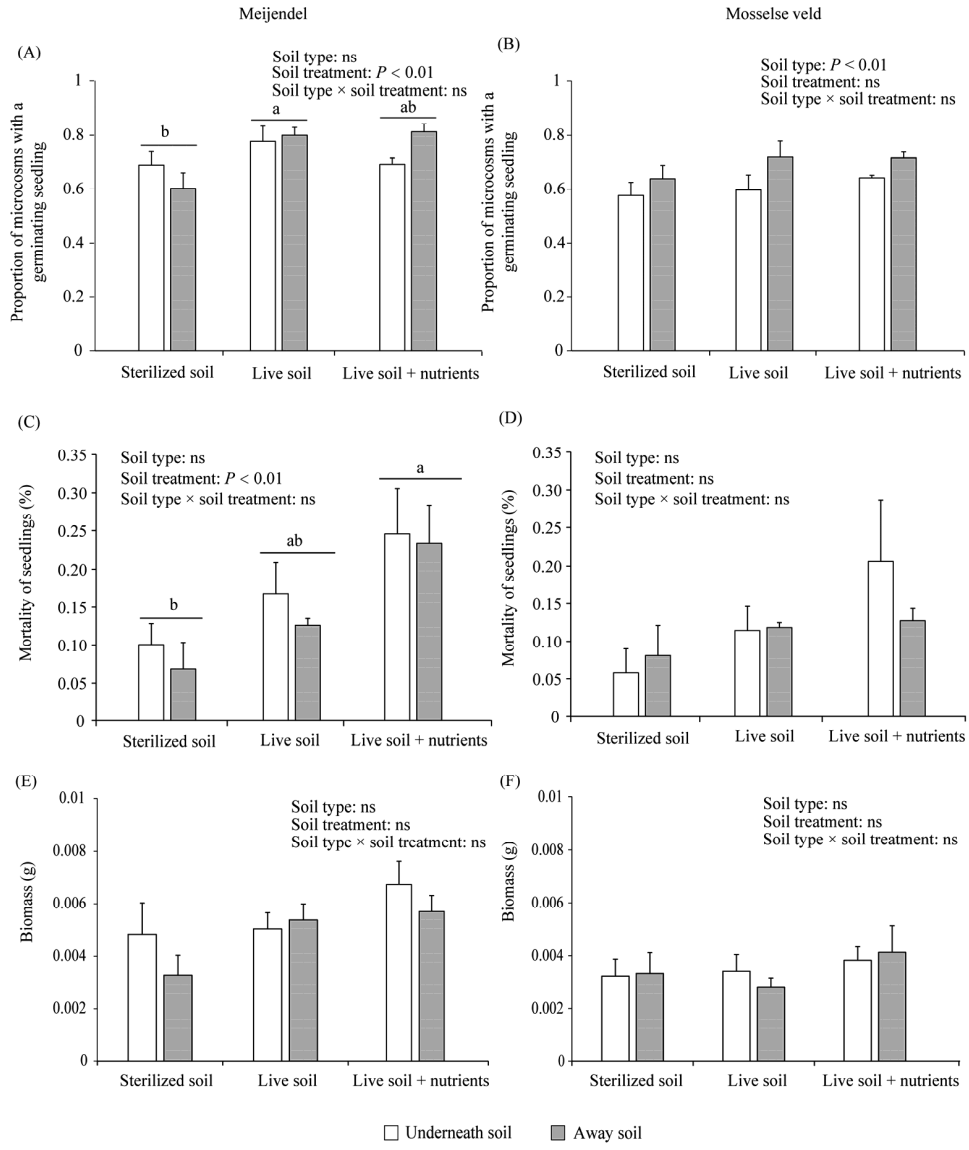

Fig. 6.5. Proportion of microcosms with a germinating seedling (A, B), seedling mortality (C, D) and plant biomass (E, F) in "underneath" and "away" soils for the different soil treatments (live soil, sterilized soil and live soil with nutrients). Soil was collected from Meijendel and Mosselse Veld. In (A) and (C) letters above each set of bars indicate significant differences between soil treatments ($P < 0.05$) based on a Tukey HSD post hoc test.

Discussion

The aim of this study was to examine soil-mediated Janzen-Connell effects of the herb *J. vulgaris* in natural grasslands. Four findings arise from this study. First, the density of rosette-bearing plants was overall lower at close distance from flowering plants than expected from null models. Second, seed germination of *J. vulgaris* was lower in soil underneath flowering plants than in the away soil, but this was only the case in soil collected from Mosselse Veld. Third, there was a density dependent self-thinning effect from rosette-bearing plants to flowering plants. This distance-based spatial pattern and the self-thinning effect appeared and became stronger during the growth season. Lastly, plant biomass did not differ neither in pairwise underneath and away soil nor in soil collected from pairwise inside and outside *J. vulgaris* patches. Overall, our study provides spatially-based evidence for conspecific distance- and density-dependent plant recruitment for *J. vulgaris* in natural grasslands, but we find no evidence that this is connected to soil conditions.

In our study, the density of rosette-bearing plants was lower than expected at close distances from flowering plants, and this negative association was present in the majority of plots at both sites. This implies a conspecific distance-dependent plant recruitment for *J. vulgaris* (Barot et al. 1999; De Luis et al. 2008; Miao et al. 2018). Such distance-dependent effect is often observed within a few meters from adult trees in forests (Swamy and Terborgh 2010; Miao et al. 2018; Malik et al. 2023). In our study, we found a negative spatial association of rosette-bearing plants and flowering plants at a much smaller distance from flowering plants. This is in line with a previous study that showed that seedlings of different herbaceous perennials exhibited a segregation pattern at centimeter scales (up to 25 cm) (De Luis et al. 2008). In the field, the flowering *J. vulgaris* plants had established at least a year earlier than rosette-bearing plants. These flowering plants could have caused abiotic (i.e. nutrient deficiency) and/or biotic changes (i.e. soil fungal communities, or allelopathic effects via chemical compounds) in the soil surrounding the plant roots and these effects can lead to negative plant-soil feedbacks (van de Voorde et al. 2012b; Kos et al. 2013, 2015a, b). *Jacobaea vulgaris* has a relative strong negative plant-soil feedback in pot experiments (van de Voorde et al. 2011). Hence we predicted that young *J. vulgaris* plants would perform worse in soils collected underneath conspecific flowering plants, and that this would eventually lead to a negative spatial association between rosette-bearing plants and flowering plants in the field. Partially following our expectation, seed germination of *J. vulgaris* was lower in the underneath soil than in the away soil, but this was only true at one of the two test locations, at Mosselse Veld. The negative effects of underneath soil on

seed germination were only detected at one site suggests that soil-dwelling natural enemies may not be the main or only reason for the observed conspecific distance-dependent plant recruitment in *J. vulgaris*. Forero et al. (2019) reported that greenhouse-derived plant-soil feedbacks were larger than and not correlated with field measured ones. Hence a strong negative plant-soil feedback in pot experiments for *J. vulgaris* does not necessarily mean that there is a strong negative plant-soil feedback in the field, and this may be an explanation for our results. In addition, recent studies suggest that plant-soil feedbacks are not operating independently but interact with multiple factors (i.e. herbivores, competition and environmental stress) under field conditions (Heinze and Joshi 2018; Beals et al. 2020; Kardol et al. 2023). Therefore, except for soil-mediated effects, there are many other potential drivers for the observed distance-dependent effects such as herbivores, seed predators and foliar pathogens (i.e. fungal pathogens) (Forrister et al. 2019; Liu et al. 2022). In our study system, caterpillars of specialized leaf chewing insect, *Tyria jacobaeae*, the cinnabar moth, feed on large plants. A spillover of herbivores such as cinnabar moth larvae on neighboring conspecific plants may also cause observed the distance-dependent effects, as previously documented (van der Meijden 1979).

Seed germination was the lowest in sterilized soil and this is somewhat unexpected and in contrast with other studies (Liu et al. 2015; Miller et al. 2019). Seed germination was also delayed in sterilized soil. The sterilized soil was somewhat compacted after being autoclaved and lower seed germination in sterilized soil may be because the structure of soil was changed. However, it is also possible that microbes in the soil beneficial for germination were killed during autoclaving, and recent studies have found that soil microbes can stimulate seed germination i.e. through germination-related enzymes (Keeler and Rafferty 2022; Cardarelli et al. 2022). Seedling mortality was not significantly different in sterilized soil and in live soil, indicating that there were limited effects of soil biota on seedling survival. However, addition of nutrients in live soil collected from Meijendel increased seedling mortality. This may because the concentration of nutrients may have cultivated more detrimental soil microbial communities in live soil collected from Meijendel in the microcosms.

In our study, we observed a density dependent self-thinning effect on *J. vulgaris* plants, as we found that rosette-bearing plants were more clustered than flowering plants. Both density-dependent competition (i.e. competition for light and space with conspecifics), herbivores and negative plant-soil feedbacks can result in this

spatial pattern. The distance-based spatial pattern and self-thinning of plants appeared and became stronger in the plots where the spatial pattern was recorded repeatedly. During the growth season, in these plots there was an increase in the density of rosette-bearing plants at the plot level, but there were even fewer rosette-bearing plants present at close distances to flowering plants. Further, the lack of a significant difference in seed bank density of *J. vulgaris* between underneath soil and away soil indicates that viable seeds are homogeneously distributed in the soil. Young seedlings are more fragile than older plants (Ailstock et al. 2010; Bezemer et al. 2018; Jevon et al. 2020). Therefore, the temporal variation in the spatial pattern that we observed suggests that conspecific negative effects exist and that they suppress the recruitment of *J. vulgaris* plants at fine scales. Except for the above mentioned herbivory and auto-toxicity, extracellular self-DNA i.e. via litter of flowering plants may also contribute to this (Mazzoleni et al. 2015a, b).

Jacobaea vulgaris has been reported to experience a strong reduction in biomass when planted in its conspecific soil in a pot experiment (van de Voorde et al. 2011). In contrast, we found biomass of *J. vulgaris* did not differ between "home" and "away" soil in both soil bioassays. Aligning with this, we did not observed that rosette-bearing plants were smaller than expected when close to flowering plants with the mark correlation function analysis. In our microcosm experiment, plants were growing in a limited amount of soil and space, and it was a short-term experiment. However, *J. vulgaris* has been found to exhibit negative plant-soil feedbacks even during the initial phase of growth (Bezemer et al. 2018; Zhang et al. 2022a). Therefore, the neutral plant-soil feedback measured in field-collected soil may not be due to the experimental design. It is important to note that soil conditioning effects by monocultures in pot experiment might be exaggerated than those observed in soil directly collected from field (Forero et al. 2019). This could potentially explain the absence of soil effects in our study. In a previous study at the Mosselse Veld grassland, Kos et al. (2013) reported that *J. vulgaris* exhibited the poorest growth in soil inoculated (1:6 of sterilized bulk soil to live field soil) with soil collected from locations with high densities of *J. vulgaris*, intermediate when inoculated with soil collected from locations with low density of *J. vulgaris* and best in pots inoculated with heterospecific soil (*Calluna vulgaris* soil). In contrast, in our study, plant growth did not differ when pots were inoculated with live soil collected from inside or outside *J. vulgaris* patches from another former arable site in the same region. Previous studies have shown that disturbance can influence the outcome of plant-soil feedbacks (Kulmatiski and Kardol 2008; Carvalho et al. 2010). Notably, *J. vulgaris* can establish well in disturbed soils

(Cameron 1935). Therefore, disturbance history may explain the lack of difference in biomass in the inside/outside patch soil in our study.

Conclusions

Overall, from our study we conclude that conspecific distance- and density-dependent plant recruitment in *J. vulgaris* are evident in natural grasslands. However, we found no evidence to support the hypothesis that this is driven by belowground differences in soil biotic properties. Nevertheless, from our study we cannot conclude that plant-soil feedbacks do not play a role in influencing plant performance and establishment at our study sites. To further explore this, future studies should conduct plant-soil feedback experiments in the field, and monitor the success of rosette-bearing plants planted directly in the soil where previously *J. vulgaris* or other plants have been grown. Such studies will significantly improve our understanding of the importance of plant-soil feedbacks under field conditions.

Author Contributions

T.M.B. and X.Y.L conceived and designed the different parts of the study. X.Y.L.. T.M.B., K.V. and S.T.E.L. developed and completed the study. X.Y.L. and C.G.G. carried out the microcosm experiments, and X.Y.L investigated the spatial distribution of *J. vulgaris*. X.Y.L. and D.H. performed the spatial pattern analysis, and X.Y.L analyzed all other data and wrote the first draft of the manuscript. All authors were involved in writing the manuscript.

Acknowledgements

We are grateful to Dunea Duin & Water company and Harrie van der Hagen for their support for the investigation in Meijendel. We thank bachelor students from the field ecology course and Johan Veenstra for measurements at the different sites, and for collecting soil samples in the field and Bowy den Braber for carrying out the patch experiment. We thank two anonymous reviewers for insightful comments and helpful suggestions. T.M.B. acknowledges funding by NWO (VIDI: grant no. 864.07.009 and VICI: grant no. 865.14.006) and Novo Nordisk (Silva Nova: grant NNF20OC0059948). X.Y.L. was funded by a Chinese Scholarship Council (CSC) grant (No.201906140116).

Supporting information

Supplementary data analysis

Detailed information of spatial point-pattern analysis testing for conspecific density-dependent effect

In the case control approach, flowering plants were seen as controls (pattern 1) and rosette-bearing plants as cases (pattern 2). "$g_{12}(r)$ represents the number of points of pattern 2 at distance r from a point of pattern 1, and $g_{22}(r)$ represents the number of points of pattern 2 at distance r from a point of pattern 2" (Getzin et al. 2008). Under the random labeling null model, $g_{12}(r) - g_{22}(r) \approx 0$, which means that rosette-bearing plants (case pattern) surround flowering plants at scale r in the same way as rosette-bearing plants surround themselves. If there would be additional clustering within the rosette-bearing plants that is independent of the pattern of flowering plants (e.g. larger gaps with suitable conditions for rosette-bearing plants establishment), "this would not be noticed by the test statistic $g_{12}(r) – g_{11}(r)$, but we would expect $g_{21}(r) – g_{22}(r) < 0$" (Getzin et al. 2008). Thus, "the outcome of $g_{12}(r) – g_{11}(r)$ can reveal if rosette-bearing plants and flowering plants follow the same overall pattern, and the outcome of $g_{21}(r) – g_{22}(r)$ can reveal if there is an additional pattern within the rosette-bearing plants that is independent of the location of the flowering plant, irrespective of whether heterogeneity is present or not" (Getzin et al. 2006; Watson et al. 2007). "Specifically, if $g_{21}(r) - g_{22}(r) < 0$ this means that the case pattern (rosette-bearing plants) shows additional aggregation which is independent from the control pattern (flowering plants) and this reflects a density-dependent thinning process" (Getzin et al. 2008).

Mark correlation function

To examine whether rosette-bearing plants are smaller than expected near flowering plants, we used the mark correlation function to analyze the diameter of rosette-bearing plants around flowering plants for the 8 plots at Meijendel where we recorded size (Illian et al. 2008; Wiegand and Moloney 2014; Velázquez et al. 2016). Wiegand and Moloney (2014) introduced mark correlation function as "summary statistics adapted for quantitatively marked patterns". The basic idea of this method is "To calculate the conditional mean of a test function $t(m_i, m_j)$ calculated from the marks m_i and m_j of two points i and j, respectively, given that they are located distance r apart." (Wiegand and Moloney 2014). In our analysis, we chose the "r-mark function" which was expressed as: $t(m_i, m_j) = m_j$ as the test function (Illian et al. 2008). In the formula, m_i means the diameter of flowering plants, and m_j means the diameter of rosette-bearing plants. The function yields a

normalized mean diameter of rosette-bearing plants at distance r away from flowering plants.

In this analysis, we used the local random labelling method within the case-control design as the null model to remove the larger-scale trends on density of rosette-bearing plants, such as environment filtering processes (Wiegand and Moloney 2014; Velázquez et al. 2016). Specifically, the random labelling method created simulations with fixed locations (coordinates) of both flowering and rosette-bearing plants from observed patterns, but randomly assigned labels of rosette-bearing plants to locations of all plants within a 1-m scale based on the aforementioned seed dispersal range of *J. vulgaris* (McEvoy and Cox 1987; Wiegand and Moloney 2014). Significant departure from local random labelling was evaluated using the 5th-lowest and 5th-highest values of 99 Monte Carlo simulations to generate approximately 95% confidence intervals. This analysis was conducted using the grid-based software Programita (Wiegand and Moloney 2014).

Table S.6.1 Soil chemistry (Mean ± SE) at Meijendel and Mosselse Veld. The raw data of soil chemistry at Meijendel were obtained from Gao (2023), who were measured soil chemistry in both the donor dune site and experimental dune site. The raw data of soil chemistry at Mosselse Veld were sourced from Kos et al. (2013), who measured soil chemistry in plots with high and low density of *J. vulgaris* plants.

	Meijendel		Mosselse Veld	
	Donor dune site	Experimental dune site	High density plots	Low density plots
P $CaCl_2$ (mg/kg)	1.40 ± 0.06	0.49 ± 0.04	1.53 ± 0.24	1.46 ± 0.33
K^+ $CaCl_2$ (mg/kg)	10.50 ± 0.71	12.90 ± 0.65	50.74 ± 6.85	32.51 ± 5.33
Mg_2^+ $CaCl_2$ (mg/kg)	11.80 ± 2.74	7.26 ± 0.31	43.49 ± 1.82	36.06 ± 3.22
NH_4^+ $CaCl_2$ (mg/kg)	1.12 ± 0.25	0.72 ± 0.17	3.25 ± 0.31	3.02 ± 0.27
NO_3^- $CaCl_2$ (mg/kg)	1.46 ± 0.25	0.93 ± 0.13	3.07 ± 0.81	4.60 ± 1.10

Table S.6.2 The number of rosette-bearing and flowering plants in each plot and field site. Note that 3 Meijendel plots (plot 9 to 11) were recorded three times in a season.

Field site	Plot ID	No. rosette-bearing plants	No. flowering plants	Total No. *J. vulgaris* plants	Month Recorded
Meijendel	plot1	162	88	250	2020.06
	plot2	505	173	678	2020.06
	plot3	520	181	701	2020.06
	plot4	82	36	118	2020.06
	plot5	189	86	275	2020.06
	plot6	335	190	525	2020.06
	plot7	337	19	356	2020.06
	plot8	115	18	133	2020.06
	plot9	420	72	492	2020.05
	plot9	1204	77	1281	2020.07
	plot9	1494	43	1537	2020.08
	plot10	621	31	652	2020.05
	plot10	1208	34	1242	2020.07
	plot10	1725	30	1755	2020.08
	plot11	466	42	508	2020.05
	plot11	948	46	994	2020.07
	plot11	1340	39	1379	2020.08
	plot12	197	205	402	2021.06
	plot13	355	343	698	2021.06
	plot14	259	146	405	2021.06
	plot15	214	146	360	2021.06
Mosselse Veld	plot16	619	261	880	2010.07
	plot17	415	363	778	2010.07
	plot18	218	252	470	2010.07
	plot19	445	301	746	2010.07
	plot20	23	63	86	2010.07
	plot21	95	120	215	2010.07
	plot22	43	80	123	2010.07
	plot23	116	161	277	2010.07
	Plot24	197	73	270	2021.06
	Plot25	261	158	419	2021.06
	Plot26	628	275	903	2021.06
	Plot27	277	96	373	2021.06

Table S.6.3 Nutrient composition of the Steiner solution.

Element	Form taken up by plants	Concentration (mg/L)
Nitrogen	NH_4^+, NO_3^-	224.51
Phosphorus	$H_2PO_4^-$	30.95
Potassium	K^+	265.45
Calcium	Ca^{2+}	259.34
Magnesium	Mg^{2+}	48.53
Sulfur	SO_4^{2-}	110.43
Iron	Fe^{2+}	5.28
Copper	Cu^{2+}	0.02
Zinc	Zn^{2+}	0.05
Manganese	Mn^{2+}	0.50
Boron	BO^{3-}	0.50
Molybdenum	MoO_4^{2-}	0.06

Table S.6.4 Number of rosette-bearing and flowering *J. vulgaris* plants per m^2, mean height of stems, bare soil and moss cover of the inside and outside of 17 *J. vulgaris* patches.

	Inside					Outside				
	No. rosette-bearing plants per m^2	No. flowering stems per m^2	Mean height of stems (cm)	Bare soil cover (%)	Moss cover (%)	No. rosette-bearing plants per m^2	No. flowering stems per m^2	Mean height of stems (cm)	Bare soil cover (%)	Moss cover (%)
Patch 1	5	3	78	5	80	2	0	/	0	0
Patch 2	6	6	70	3	30	0	0	/	10	8
Patch 3	11	15	89	5	80	0	0	/	0	0
Patch 4	7	17	76	15	60	5	0	/	5	20
Patch 5	3	15	65	5	20	12	0	/	7	0
Patch 6	1	6	77	0	10	4	0	/	0	8
Patch 7	48	11	69	0	80	5	0	/	0	0
Patch 8	22	8	84	0	20	1	0	/	2	0
Patch 9	13	4	65	0	30	9	0	/	0	7
Patch 10	24	7	71	0	0	32	0	/	0	15
Patch 11	5	22	82	0	75	7	0	/	0	6
Patch 12	8	13	79	0	10	1	0	/	0	5
Patch 13	1	13	81	0	0	0	0	/	0	0
Patch 14	4	7	69	20	15	0	0	/	0	0
Patch 15	12	18	80	0	0	0	0	/	0	0
Patch 16	11	9	71	0	0	12	0	/	0	0
Patch 17	4	19	85	0	0	3	0	/	0	20

Table S.6.5 Results of a generalized linear mixed model and a two-way ANOVA testing soil type (underneath or away), soil treatment (sterilized soil, live soil or live soil with addition of nutrients) and their interaction on seed germination, seedling mortality and plant biomass of *J. vulgaris* at each site. Presented are degrees of freedom (df), Likelihood-Ratio Chi-squares or F-values and *P* values. ** indicates significant differences at $P < 0.01$. For seed germination, the formula of the generalized linear mixed model is: germination (yes/no) ~ soil type × soil treatment + (1| ID of flowering plants). For seedling mortality and biomass, the formula of the two-way ANOVA is: seedling mortality / biomass ~ soil type × soil treatment.

		Meijendel			Mosselse Veld		
		df	χ^2	*P*	df	χ^2	*P*
Seed germination	Soil type	1	0.26	0.61	1	7.43	0.01**
	Soil treatment	2	9.65	0.01**	2	5.31	0.07
	Soil type × Soil treatment	2	4.86	0.09	2	0.40	0.82
		df	F	*P*	df	F	*P*
Seedling mortality	Soil type	1, 12	0.73	0.41	1, 12	0.25	0.62
	Soil treatment	2, 12	7.29	0.01**	2, 12	2.73	0.11
	Soil type × Soil treatment	2, 12	0.06	0.94	2, 12	0.83	0.46
		df	F	*P*	df	F	*P*
Biomass	Soil type	1, 235	2.80	0.06	1, 229	1.42	0.24
	Soil treatment	2, 235	0.53	0.47	2, 229	0.92	0.34
	Soil type × Soil treatment	2, 235	0.70	0.50	2, 229	0.44	0.65

Table S.6.6 Mean (± SE) of individual shoot dry mass, total shoot dry mass, total root dry mass and results of a pairwise t-test testing soil type (inside or outside of patches with high densities of *J. vulgaris*) on the growth of *J. vulgaris* plants. Presented are degrees of freedom (df), t-values and *P* values.

	Inside of the patches	Outside of the patches	df	t	*P*
	Mean ± SE	Mean ± SE			
Individual shoot dry mass (g)	0.82 ± 0.03	0.76 ± 0.04	16	1.41	0.18
Total shoot dry mass (g)	2.46 ± 0.10	2.27 ± 0.12	16	1.40	0.18
Total root dry mass (g)	3.50 ± 0.20	3.14 ± 0.23	16	1.48	0.16

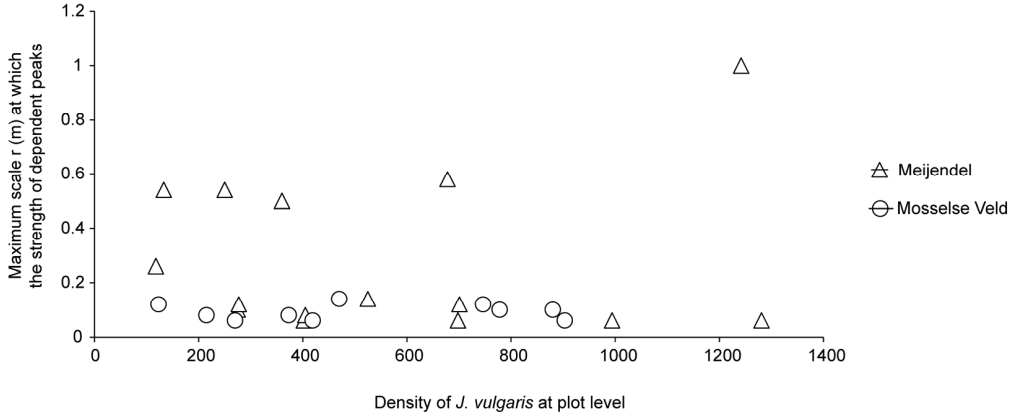

Fig. S.6.1. The relationship between maximum scale (m) at which the strength of density dependent peaks and density of *J. vulgaris* plants at plot level. There was no significant linear relationship.

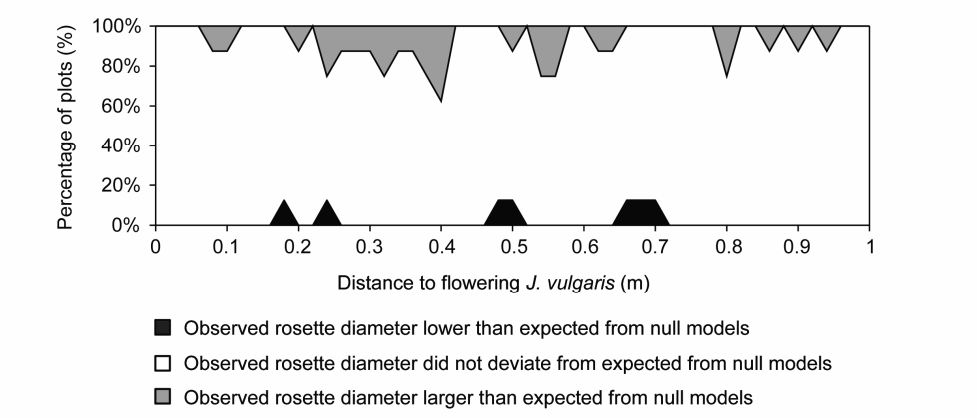

Fig. S.6.2. Percentage of plots with mean diameter of rosette-bearing plants smaller, equal or larger than the expected diameter of rosette-bearing plants from null models in June 2020 at 8 plots in Meijendel. The black area indicates the percentage of plots where the diameter of rosette-bearing plants was smaller than the expected diameter (values below the lower limits of the 95% confidence interval). The white area indicates the percentage of plots where the diameter of rosette-bearing plants as equal as the expected diameter (values in between the 95% confidence interval). The light grey area indicates the percentage of plots where the diameter of rosette-bearing plants was larger than the expected diameter (values above the higher limits of the 95% confidence intervals).

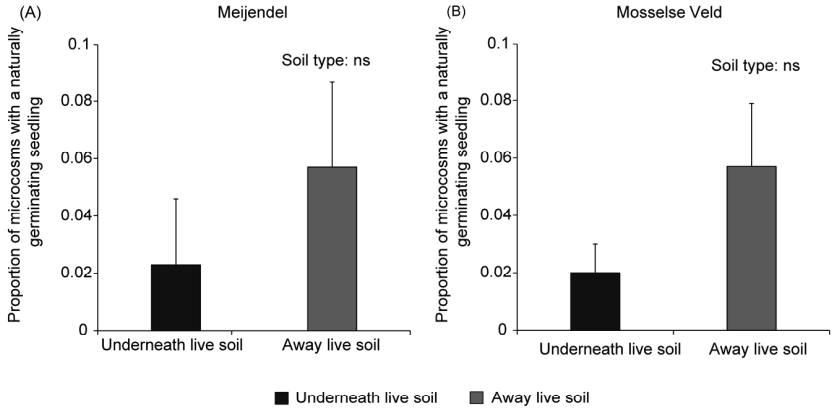

Fig. S.6.3. Proportion of microcosms with a naturally germinating *J. vulgaris* seedling (seed bank) grown in the underneath and away live soil in the Meijendel (A) and in the Mosselse Veld (B). There was no significant difference between soil treatments at both sites.

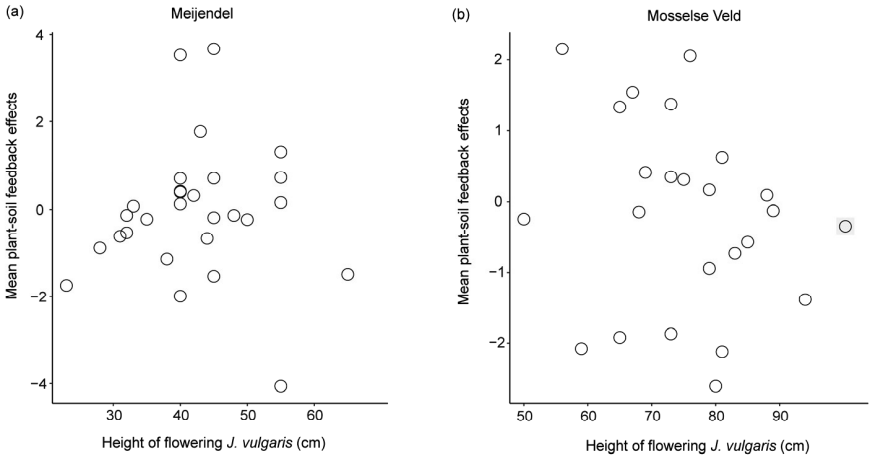

Fig. S.6.4. The relationship between mean plant-soil feedback effects and the height of flowering *J. vulgaris* plants in the Meijendel (A) and in the Mosselse Veld (B). There was no significant linear relationship at both site.